WS2021/22

PPBphys2

Doppler-free Saturation Spectroscopy of Rubidium

Manuel Lippert - Paul Schwanitz

Group 11

Information

Day	21.09.2021
Place	BGI | 3.0.09
Supervisor	Sanchayeeta Jana
Group Nr.	11
Participant	Manuel Lippert (Manuel.Lippert@uni-bayreuth.de)
	Paul Schwanitz (Paul.Schwanitz@uni-bayreuth.de)

Contents

1 Introduction

Spectroscopy is a very important tool to discover the structure from atoms and molecules. With the help of that tool, the physicists discover the spectral lines of the H-atom. This is where spectroscopy began.
The research in this are also helps to discover things like fine and hyperfine structure. What finaly leads to Quantum mechanics.
Furthermore, spectroscopy is also very useful tool for other areas of science like chemistry or biology. In this areas spectroscopy helps to analyze probes and provides information about which materials the probe is made of.
So the aim of this Experiment is to get in contact with experimental atom and nucleus physics by means of Doppler-free Saturation Spectroscopy of Rubidium.

2 Theoretical background

2.1 Saturation spectroscopy in general

With saturation spectroscopy enables us to see the hyper fine structure, because with this method it is theoretical possible to bypass the doppler effect.
By saturation spectroscopy a laser (pump beam) beam will pass a gas sample (with doppler widened absorption transitions). That caused a stimulation of specific atoms, depending from there speed.

Vice versa to the pump beam another laser beam with the same frequency (probe beam) will also pass the gas sample.

If now a photon is absorbed, the atom must have a speed component (v_z parallel to the laser beams) in the interval:

$$v_\mathrm{z} \pm \Delta v_\mathrm{z} = \frac{\omega - \omega_0 \pm \delta\omega_\mathrm{n}}{k} \tag{2.1}$$

In this connection:

- $\delta\omega_\mathrm{n}$ is the homogeneous line width.
- Δv_z is the width of the hole in the occupation distribution.
- ω is the frequency of the laser.
- ω_0 is the resonance frequency of the wanted transition.

Because many atoms are stimulated, the probe beam hits barley atoms that can be stimulated. For this reason we obtain the occupation distribution $N(v_\mathrm{z})$ and the adsorption profile $\alpha(\omega)$. For this experiment the laser frequency is so chosen, that the fit with the resonance frequency of the wanted transition (Bleiner, ????).

2.2 Preparatory questions

1. Nuclear spin Because the isotopes have a different nuclear structure and the spin depends on that structure, the spins are different. Below the quantum numbers of the basic condition and the fist two stimulated conditions:

isotope	basic condition	first stimulated condition	second stimulated condition
Rb-85	$5^2S_{\frac{1}{2}} \Rightarrow F = 2, 3$	$5^2P_{\frac{1}{2}} \Rightarrow F = 2, 3$	$5^2S_{\frac{3}{2}} \Rightarrow F = 1, 2, 3, 4$
Rb-87	$5^2S_{\frac{1}{2}} \Rightarrow F = 1, 2$	$5^2P_{\frac{1}{2}} \Rightarrow F = 1, 2$	$5^2S_{\frac{3}{2}} \Rightarrow F = 0, 1, 2, 3$

Table 2.1: Quantum numbers of Rb-85 and Rb-87

2. Important terms

a) Natural line width
The natural line width is only the result of the finite beam duration. So it is the smallest line width you can measure (Demtröder, 2015).

b) Doppler broadening
If a stimulated atom moves with a speed component v_z the light who is emitted by this atom and has a wave vector component k_z is subject to the doppler effect. Because the atom movement is statistical and depends on the temperature of the probe the doppler broadening also depends on the temperature (Demtröder, 2015).

$$\Delta\nu_D = \frac{2\nu_0}{c}\sqrt{\ln(2)\frac{2k_BT}{m}} = \frac{2\nu_0\hat{v}}{c}\sqrt{\ln(2)} \text{ with } \hat{v} = \sqrt{\frac{2k_BT}{m}}, \tag{2.2}$$

$$\Delta\nu_D = 2\sigma\sqrt{\ln(2)} \Rightarrow \sigma = \frac{2\nu_0\hat{v}}{c} \Leftrightarrow \hat{v} = \frac{\sigma c}{2\nu_0} \tag{2.3}$$

c) Homogeneous/inhomogeneous widening
Is the probability for emission and absorption equal, so is the line homogeneously widened. If not, it is inhomogeneously broadened (Demtröder, 2011).

d) Saturation widening
The line profile will be changed caused by a change of the occupation number of the transition. The pump beam causes a saturation of the occupation density and this leads to a line widening (Demtröder, 2011).

3. Cross-over resonances Cross-over resonances are additionally occurring resonance line between tow lamp dips. They are caused by an overlap of the doppler broadened signals. The following applies to the frequency:

$$f_\mathrm{c} = \frac{f_1 + f_2}{2} \tag{2.4}$$

4. Beam splitter and $\lambda/2$ plate The $\lambda/2$ plate and filter wheel in connection with the first beam polarizing splitter is for the adjustment of the intensity distribution between the Pump beam and the probe beam. The second polarizing beam splitter is used to decouple the probe beam and couple the pump beam.

5. Hyperfine structure The Hyperfine constant can be calculated with the following formular:

$$\Delta E_\mathrm{HFS} = \frac{a}{2}[F(F+1) - J(J+1) - I(I+1)] \tag{2.5}$$

In this con a is the Hyperfine constant.

$$a = \frac{g_\mathrm{I}\mu_\mathrm{k}}{\sqrt{J(J+1)}} \tag{2.6}$$

$$\mu_\mathrm{k} = \frac{eh}{2m_\mathrm{p}} = 5.0510 \cdot 10^{-27} \tag{2.7}$$

g_I is the Lande-factor.
The possible transitions are determined by the selection rules of the hyperfine structure (Demtröder, 2015):

- $\Delta F = 0, \pm 1$
- $\Delta J = 0, \pm 1$
- $\Delta L = \pm 1$

3 Protocol

Adjustment for measurement

We adjust the test setup after instruction of the supervisor with the adjusting tip. For that we make sure to take two points for two mirrors that are as far as possible away from the specific mirror.

Chanels

Input	Output	Description
ai0	RF Output	balance of reference beam and measurement beam
ai1	Monitor +	measurement beam
ai3	Monitor -	reference beam
ai4	PD2 Output	signal of fabry-pérot-interferometer

For our files we have taken the name: *MesN_TempY_ZPeaks* there N is number of the measurement/id and Y is the temperature 24 °C, 38 °C, 56.2 °C without the unit and Z is the number to identify the peak with the values all, 1, 2, 3, 4 which is number from left to right. To every measurement we save a .dat-file and a .bmp-file on our usb-stick. We also used always the act-value and not the set-value for measurement.

Measurement

- **Temperature:** 24 °C
  Filename: *date+time_group11_MesN_Temp24_ZPeak.dat and .bmp*
  N from 1 to 5, act-value: 24 °C
- **Temperature:** 38 °C
  Filename: *date+time_group11_MesN_Temp38_ZPeak.dat and .bmp*
  N from 6 to 10, act-value: 40 °C
- **Temperature:** 56.2 °C
  Filename: *date+time_group11_MesN_Temp38_ZPeak.dat and .bmp*
  N from 11 to 15, act-value: 60 °C
- **Distance fabry-pérot-interferometer:** 72.5 cm+36 cm+43 cm=151.5 cm
  measured with tape measure

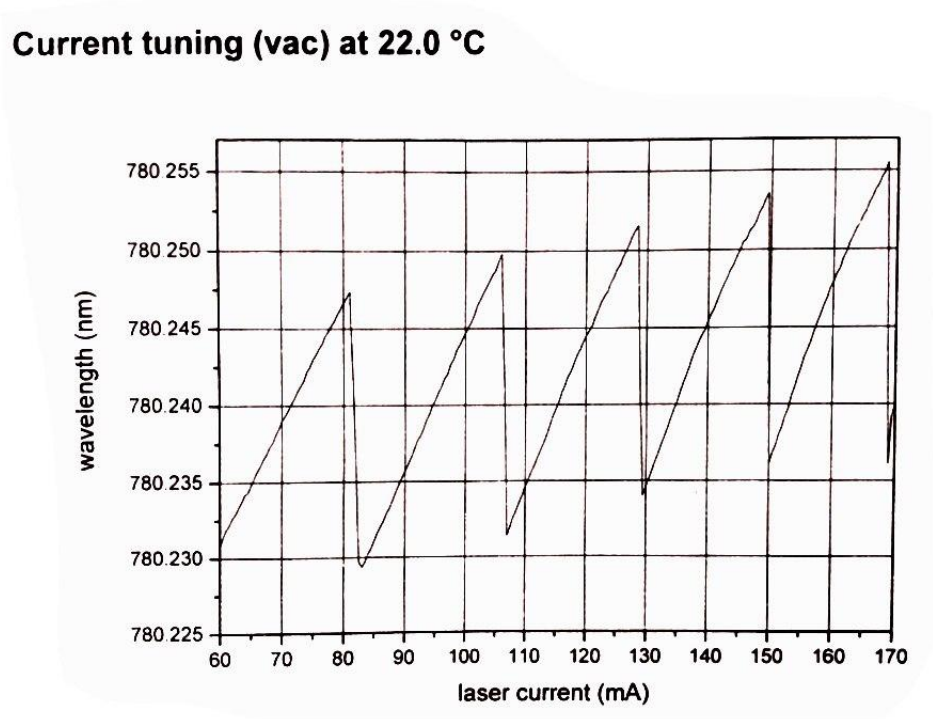

Figure 3.1: Currunt Tuning at 22 °C from laser instructions

4 Evaluation

We have chosen to take the measured data for 24 °C, because the reference beam and the sample beam have had the best alignment. It seems also in this data the observation of the height of the lamb dips and the width of the lines would be much easier as in the other temperatures.

4.1 Freeing Absorption Spectrum from Trend and identify Lines

Now we want to free the spectrum from any trend for that the fit a linear function on the spectrum of the reference beam and subtract the fit from the sample beam and reference beam. It is worth mentioning that we have moved the reference beam spectrum down to the niveau of the sample beam spectrum and after that we fitted the linear function. In fig. 4.1 we can see the absorption spectrum with trends and the linear fit and in fig. 4.2 the spectrum without trends. The fit is managed with the function polyfit of the numpy-module in python. We did also cut the data so that we can clearly see the four peaks without any jumps in mode.

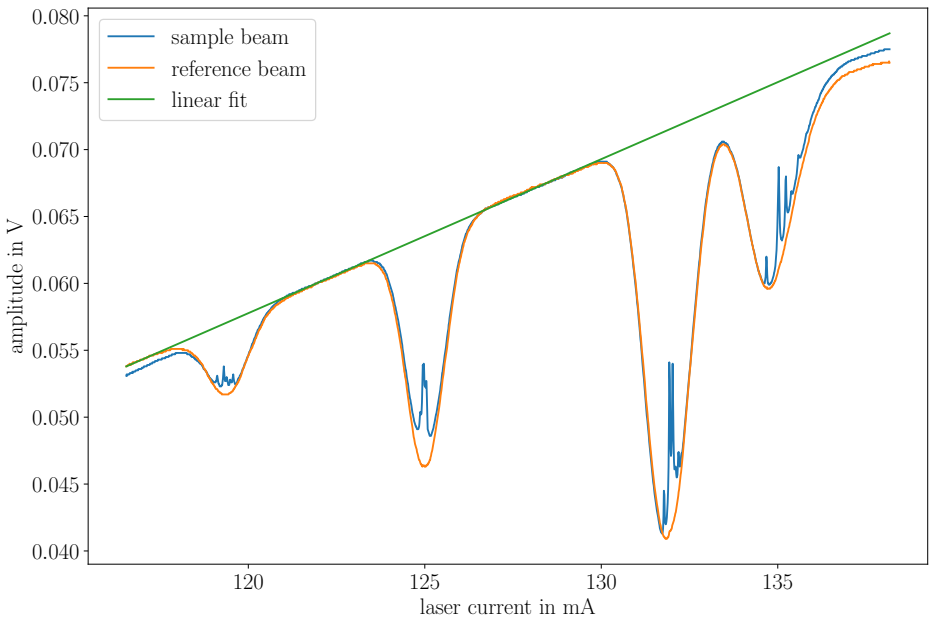

Figure 4.1: absorption spectrum with trends

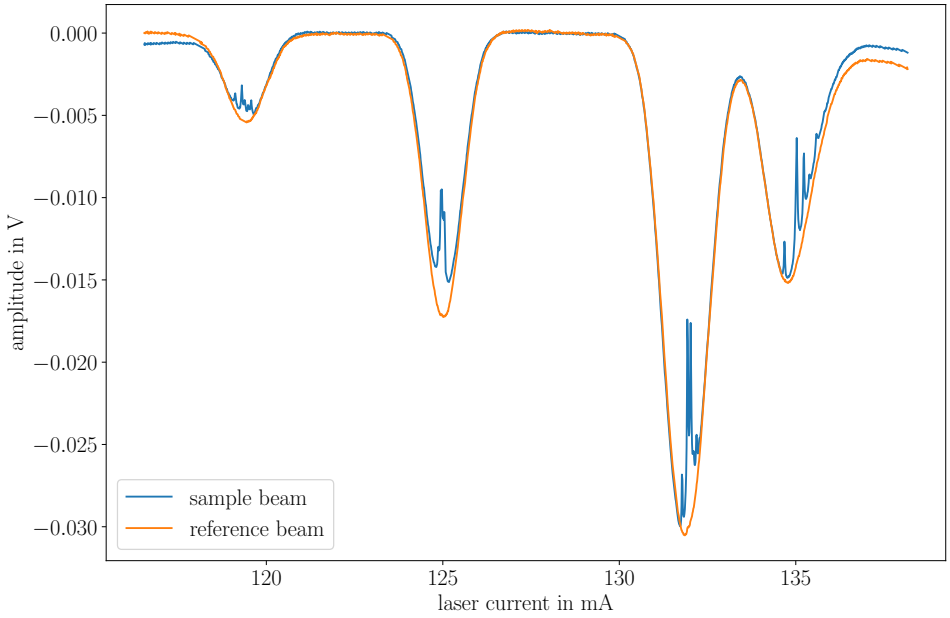

Figure 4.2: absorption Spectrum without trends

We applied the same procedure on the data of the fabry-pérot and see clear in fig. 4.3 that the signal is not very stable, but this is not from interest for the upcoming evaluation because we need only the distance between to peaks.

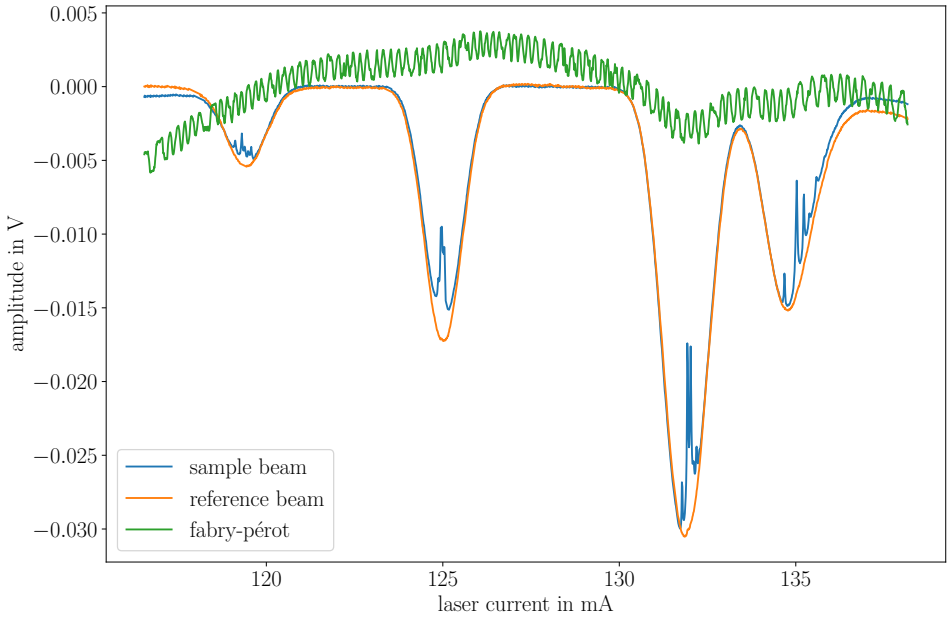

Figure 4.3: absorption spectrum without trends all channels

Identfication considering intensity and order

To identify the lines of the spectrum we used the current wavelength curve (look fig. 3.1) to convert the laser current to the wavelength. To do this we convert the fig. 3.1 into a csv-file using python. For that we measured roughly the points of the peaks from 105 mA to 150 mA (because that is the area of interest) and calculated a basic linear function of the form $y = mx + t$ between them (look fig. 4.4). Then we obtain three separate linear functions that can transform our data in the corresponding wavelength in the specific area of the current wavelength curve.

	1	2	3	4
laser current/mA	107.0	128.5	129.5	149.5
wavelength/nm	780.23125	780.25125	780.234	780.2535

Table 4.1: point used for recreating current wavelength curve

area	m/$\frac{\text{nm}}{\text{mA}}$	t/nm
$1 \rightarrow 2$	0.00093	780.132
$2 \rightarrow 3$	-0.01725	782.468
$3 \rightarrow 4$	0.00097	780.108

Table 4.2: linear functions of the current wavelength curve

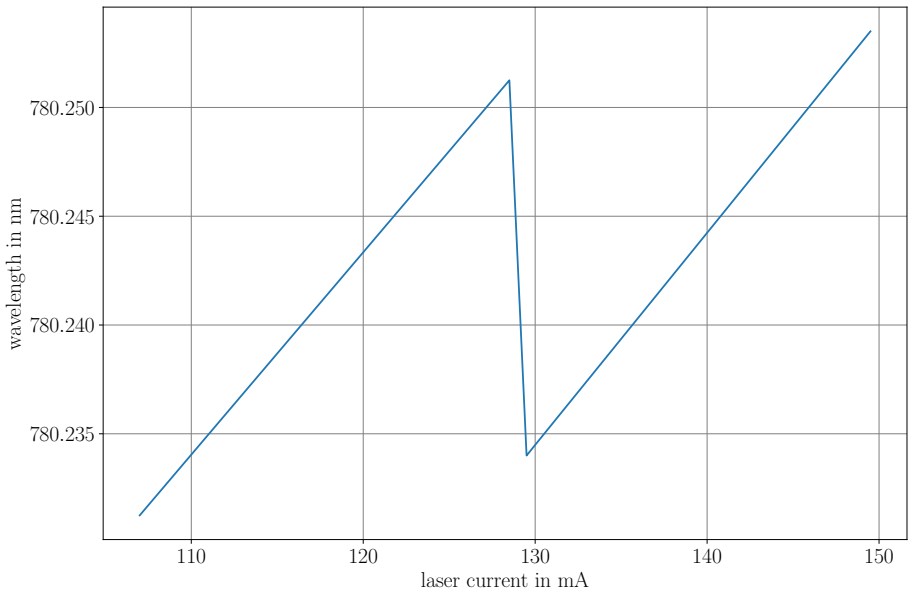

Figure 4.4: cut current wavelength curve from 105 mA to 150 mA using python

From the csv-file we can easily find our value for the peaks of the reference beam and convert them into the corresponding wavelength. Then we compared the measured wavelength with the literature (Steck, 2013, 2015) there F are the quantum number of the $5^2S_{1/2}$-state.

peak order	laser current/mA	wavelength measured/nm	wavelength literature/nm	deviation/nm	isotope	F
1	119.4429	780.243	780.233	0.010	^{87}Rb	1
2	125.0267	780.248	780.238	0.010	^{85}Rb	2
3	131.8581	780.236	780.244	0.008	^{85}Rb	3
4	134.7829	780.239	780.246	0.007	^{87}Rb	2

Table 4.3: identification by intensity and order

Because ^{85}Rb have to be isotope with the highest occurrence we can clearly identify the highest peaks of the absorption spectrum as the one of ^{85}Rb. In addition to that we can conclude that the measured data have some kind of bias, roughly 0.010 nm, in each area of the current wavelength curve of the laser.

4.2 Distance between Energy Levels

Current Wavelength Curve

As mentioned in chapter 4.1 we already have transformed all data into the wavelength using the current wavelength curve. Because of that the order of the peaks has changed to 3 4 1 2. The next step is to transform the wavelength into the frequency using the formula $\nu = \frac{c}{\lambda}$, where c is the speed of light in vacuum. The result can be seen in fig. 4.5.

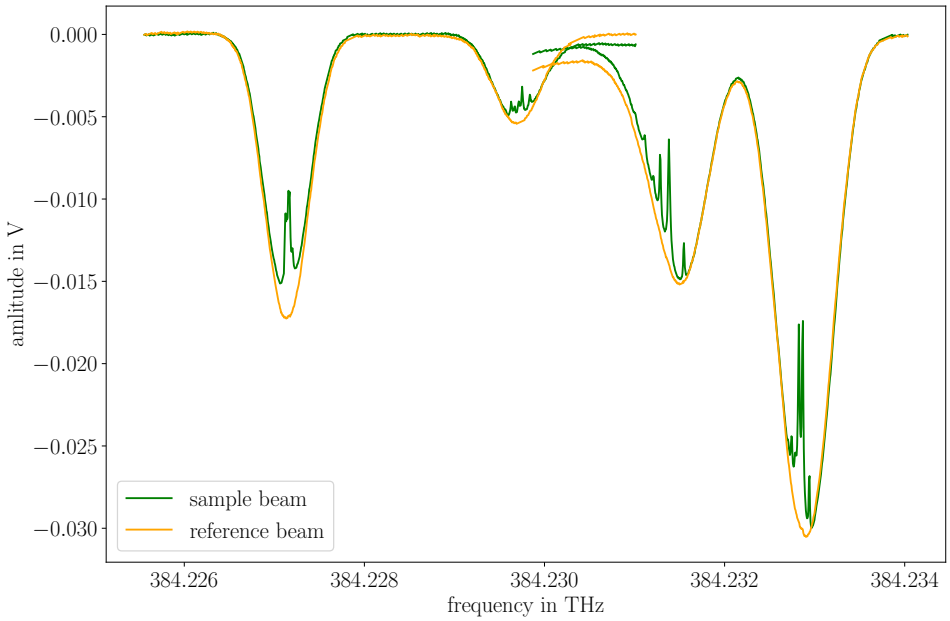

Figure 4.5: absorption spectrum after transformation to frequency

One can also see the occurrence of overlapping in fig. 4.5 that is caused by the transformation from the laser current to the wavelength. It is possible to erase the overlapping lines from the data but for this evaluation it is necessary. By using the same method as in chapter 4.1 to identify the peaks we obtain distance as followed:

peak area	$d_{\text{current}}/\text{THz}$
$2 \to 1$	0.00256
$1 \to 4$	0.00181
$4 \to 3$	0.00140

Table 4.4: distances between the energy levels using current wavelength curve

Fabry-Pérot Interferometer

To calculate the distance of the energy level we start using the function of the Fabry-Pérot interferometer and insert the measured length d:

$$\Delta\omega_{\text{FSR}} = \frac{c}{2nd} \overset{n=1}{=} \frac{c}{2d} \overset{d=1.515\,\text{m}}{=} 98.9\,\text{MHz} \tag{4.1}$$

In the trendfree line of the interferometer we can count from 117.0455 mA to 137.6816 mA an amount of 97 maxima peaks what gives as relation:

$$\frac{97 \cdot \Delta\omega_{\text{FSR}}}{137.6816\,\text{mA} - 117.0455\,\text{mA}} = 0.465\frac{\text{GHz}}{\text{mA}} \tag{4.2}$$

This means that 1 mA correspond to 0.465 GHz. In following we use the table 4.3 from chapter 4.1 for the information of the current for each peak and take the difference of them. That gives us in comparsion with the calculated data from table 4.4:

peak area	difference/mA	$d_{\text{interferometer}}/\text{THz}$	$d_{\text{current}}/\text{THz}$
$1 \to 2$	5.5838	0.00260	0.00256
$2 \to 3$	6.8314	0.00318	—
$3 \to 4$	2.9248	0.00136	0.00140

Table 4.5: distance between the energy levels using Fabry-Pérot interferometer and comparison to usage of current wavelength curve

In table 4.5 we can clearly see that both methods are equal in evaluation.

4.3 The real ratio of the rubidium isotopes

Now we calculate the ratio of each isotope by identifying the area under every peak. For that we are fitting the gaussian distribution for each peak of our data for the reference beam absorption spectrum. We take the current axis because for the ratio it does not matter which axis we use. Furthermore, we use the data that is freed from any trends (look fig. 4.2).Then the fitting function has the form of:

$$y = a \cdot \exp\left(-\left(\frac{(x-b)}{\sqrt{2}c}\right)^2\right) \tag{4.3}$$

b is here the x-value of each peak that we have already obtained in table 4.3. We get with the curve$_f$it of scipy.optimize package from python:

peak	a/V	b/mA	c/mA
1	-0.00539	119.4429	0.57669
2	-0.01742	125.0267	0.52976
3	-0.03085	131.8581	0.62443
4	-0.01462	134.7829	0.74425

Table 4.6: fitting data for each peak

In figure 4.6 is shown how each gaussian fit looks for each peak.
With the parameter we calculated above we are now able to determine the area under each curve of each peak with the following relation:

$$\int_{-\infty}^{\infty} \exp\left(-k(x-\mu)^2\right) dx = \sqrt{\frac{\pi}{k}} \xrightarrow{\mu=b,\ k=\frac{1}{2c^2}} \int_{-\infty}^{\infty} a \cdot \exp\left(-\left(\frac{(x-b)}{\sqrt{2}c}\right)^2\right) = a\sqrt{2\pi c^2} \tag{4.4}$$

This expression gives us then the area as follows:

peak	isotope	area/$1 \cdot 10^{-6}$ W
1	^{87}Rb	-7.79
2	^{85}Rb	-23.13
3	^{85}Rb	-48.29
4	^{87}Rb	-27.27

Table 4.7: area under the curve of each peak

The area under the peaks is proportional to the amount of atoms of each isotope in the gas what gives us:

$$^{85}Rb = \frac{23.13 + 48.29}{7.79 + 23.13 + 48.29 + 27.27} = 0.671 \Rightarrow {}^{87}Rb = 0.329 \tag{4.5}$$

Meaning that in our probe there is 67.1 % ^{85}Rb and 32.9 % ^{87}Rb which compared to the literature (Steck, 2013, 2015) (72.2 % ^{85}Rb and 27.8 % ^{87}Rb) shows that the assumption from chapter 4.1 to take the intensity into account was correct.

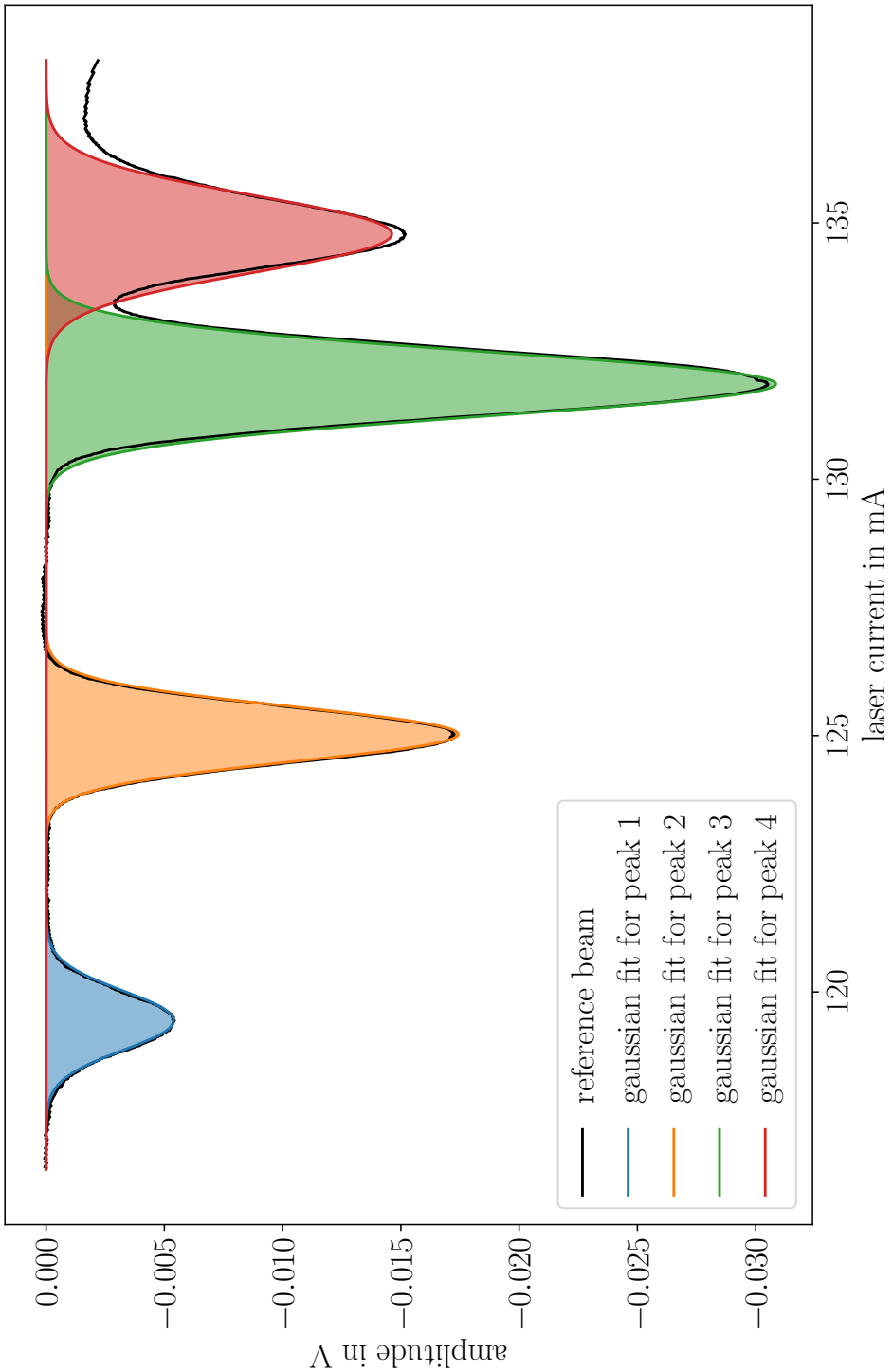

Figure 4.6: gaussian fit for each Peak of the reference beam spectrum

4.4 Hyperfine Dips

Firstly we want to show all absorption dips separately starting with peak 1 and ending with peak 4.

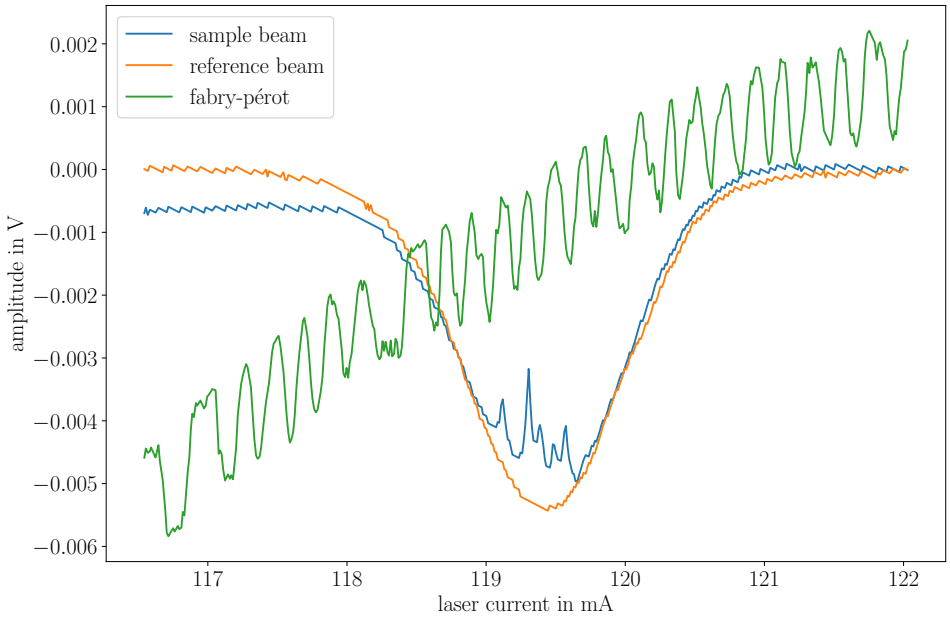

Figure 4.7: absorption spectrum of peak number 1

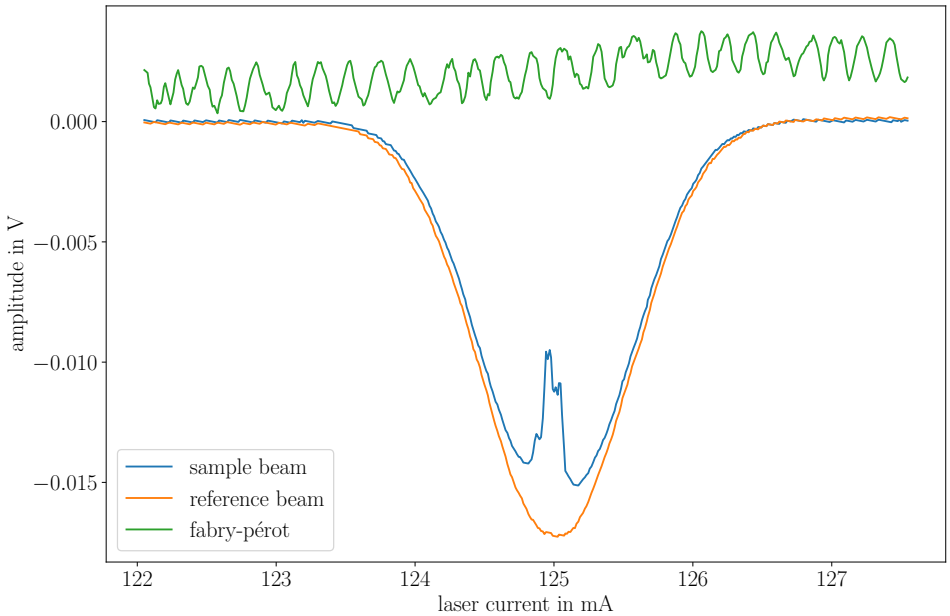

Figure 4.8: absorption spectrum of peak number 2

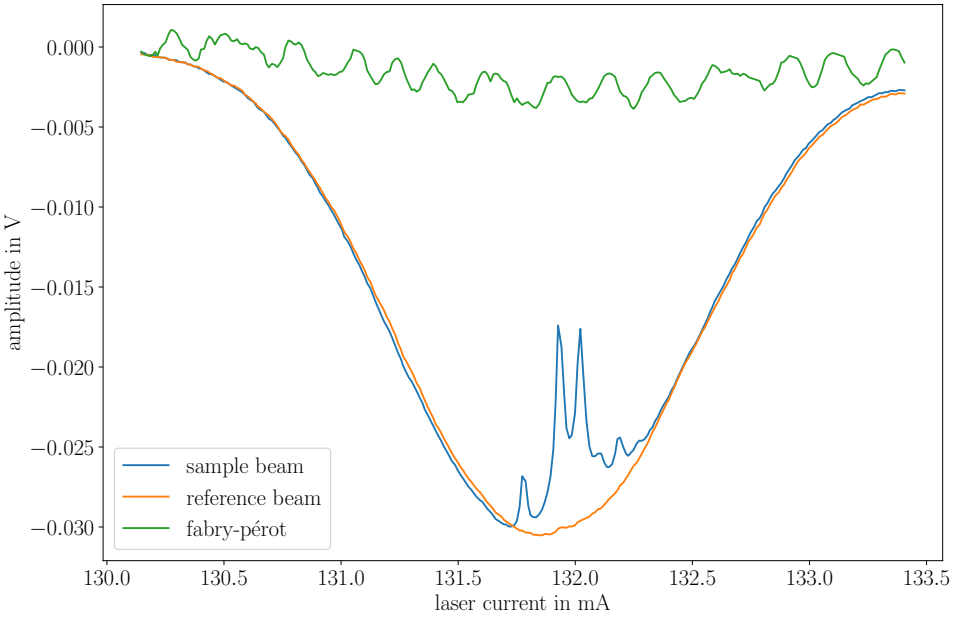

Figure 4.9: absorption spectrum of peak number 3

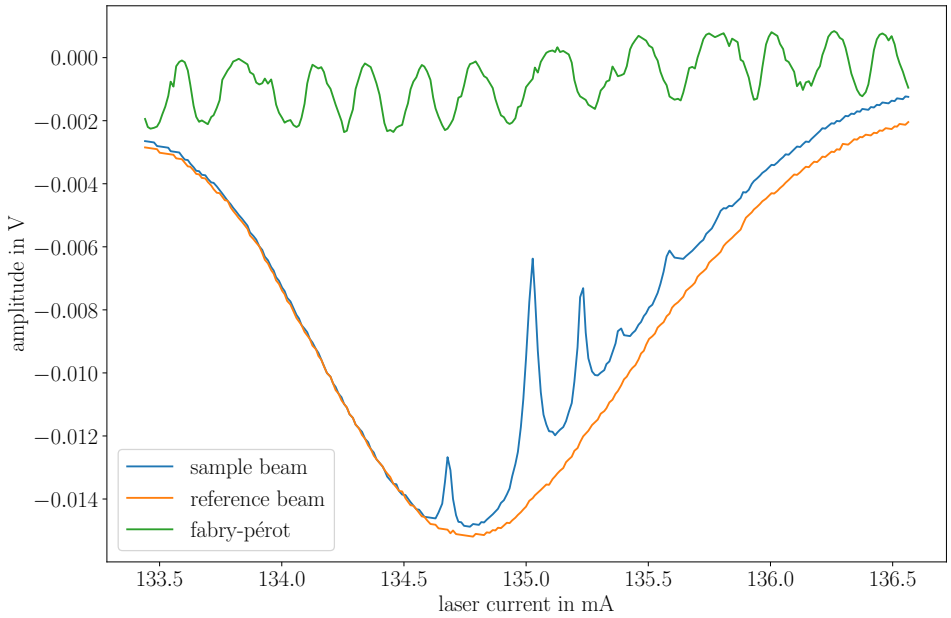

Figure 4.10: absorption spectrum of peak number 4

It was chosen to use the peak number 3 because there are the hyperfine dips clearly visible. Its the isotope ^{85}Rb. For the upcuming calculation we will use the measured data of peak 3 only because of that we have had an offset in our data from $z_{\text{off}} = 0.072\,\text{V}$ and have to transform the laser current again like in chapter 4.1 into wavelength and frequency. The fit of the Lorentz curve (lorentzian) was achieved with the function:

$$y = \frac{ac^2}{(x-b)^2 + c^2} - d \tag{4.6}$$

By observing the formula of the fit it gets clear that a is nothing else as the laser current value and b the amplitude of each hyperfine dip peak. From that conclusion we get for the hyperfine peaks numbered from left to right:

hyperfine peak	a/mA	a/nm	a/THz	b/V	c/mA	d/V
1	131.8489	780.236290	384.232907	-0.0269	-0.0266	-0.032
2	132.0006	780.236438	384.232834	-0.0169	-0.0285	-0.032
3	132.0778	780.236513	384.232797	-0.0177	-0.0325	-0.032
4	132.1607	780.236594	384.232757	-0.0254	-0.0680	-0.032
5	132.2349	780.236667	384.232722	-0.0243	-0.0613	-0.032

Table 4.8: fitting data for each hyperfine dip

Furthermore the lorentzian fit for each dip can be seen in fig. 4.11.
It is clear that there are more dips than possible hyperfine transition. In case of ^{85}Rb each dip represents a transition from energy levels $F = 3$ of the state $5^2S_{1/2}$ to a different energy level of the $5^2P_{3/2}$ state with quantum number F', in short: $F = 3 \to F'$. With the selection rule of the hyperfine transition ($\Delta F = 0, \pm 1$) we obtain that there should be only three dips visible ($F' = 2, 3, 4$) the remaining dips come from cross over resonances. For Comparison with the literature (Steck, 2013) we calculate the distance between the dips using table 4.8 and obtain:

dip area	distance measured/MHz	distance literature/MHz	transition $F_1' \leftrightarrow F_2'$
$1 \to 2$	73.00	63.38	$2 \leftrightarrow 3$
$2 \to 5$	114.00	120.99	$3 \leftrightarrow 4$

Table 4.9: distance between the selected dips

The Comparison with the literature shows us that indeed the peek 3 should be ^{85}Rb as we assumed in chapter 4.1 and 4.3. The difference between literature and measurement could have the same cause as the difference in chapter 4.1.

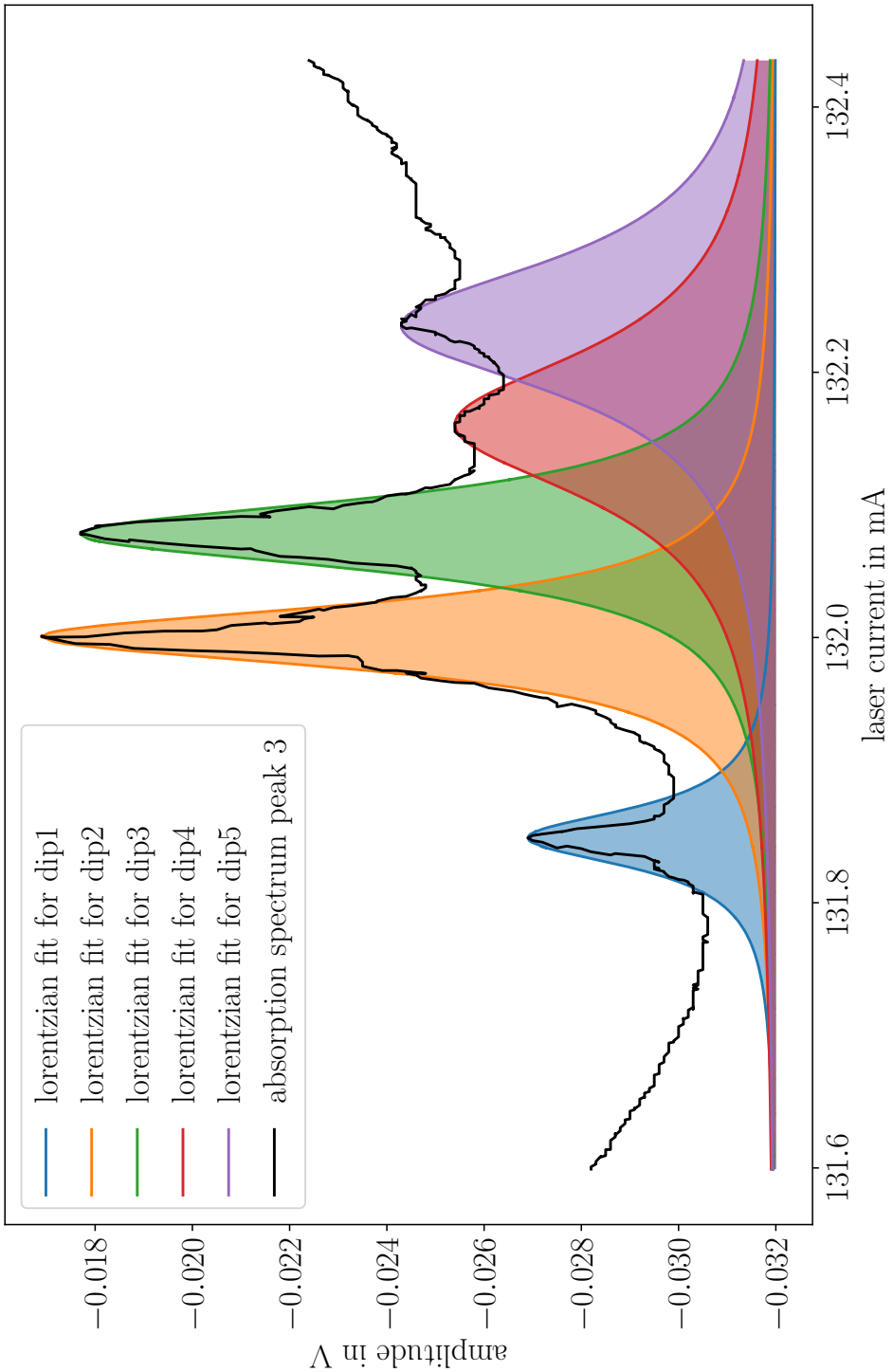

Figure 4.11: lorentzian fit for each dip of peak 3

4.5 Hyperfine constant

In the following we use the equation 4.7 to calculate the hyperfine constants.

$$\Delta E_{\mathrm{HFS}} = \frac{a}{2}[F(F+1) - J(J+1) - I(I+1)] \tag{4.7}$$

We know the Energy difference and the Quantum numbers of the transitions from table 4.9. So we can rewrite the equation:

$$a = \frac{2(\Delta E)}{F_2(F_2+1) - F_1(F_1+1)} \qquad \text{mit} \quad \Delta E = h \cdot \Delta\nu \tag{4.8}$$

After we put in the values we get the following results:

transition	a in 10^{-26} J	literature: a in 10^{-26} J
$2 \leftrightarrow 3$	1.612	1.400
$3 \leftrightarrow 4$	1.888	1.840

Table 4.10: hyperfine constants

The literature value of a is computed by the literature value of $\Delta\nu$ from table 4.9. The difference of one value cloud have the same problem as mentioned in chapter 4.4.

4.6 Gas Temperatures

To calculate the gas temperature we can use the formula

$$\Delta\nu_{\mathrm{D}} = \frac{2\nu_0}{c}\sqrt{\ln(2)\frac{2k_{\mathrm{B}}T}{m}} = \frac{2\nu_0\hat{v}}{c}\sqrt{\ln(2)} \text{ with } \hat{v} = \sqrt{\frac{2k_{\mathrm{B}}T}{m}}, \tag{4.9}$$

where $\Delta\nu_{\mathrm{D}}$ is the doppler width, ν_0 the frequency of the peak, $\hat{v}$ the most probable velocity, k_{B} the Boltzmann constant, T the temperature and c the speed of light in vacuum. First we have to calculate the doppler width or most probable velocity. For that we are fitting a gaussian on the spectrum of the reference beam as in chapter 4.6 with the form:

$$y = y(\nu_0)\exp\left(-\left(\frac{\nu-\nu_0}{\sigma}\right)^2\right) \tag{4.10}$$

With the value of σ one can calculate $\Delta\nu_{\mathrm{D}}$ or $\hat{v}$ as following:

$$\Delta\nu_{\mathrm{D}} = 2\sqrt{\ln(2)}\sigma \Rightarrow \sigma = \frac{\nu_0\hat{v}}{c} \Leftrightarrow \hat{v} = \frac{\sigma c}{\nu_0} \tag{4.11}$$

After that one can obtain T and the mean velocity $\overline{v}$:

$$\hat{v} = \sqrt{\frac{2k_{\mathrm{B}}T}{m}} \Leftrightarrow T = \frac{m}{2k_{\mathrm{B}}}\hat{v}^2 \text{ and } \overline{v} = \sqrt{\frac{8k_{\mathrm{B}}T}{\pi m}} = \sqrt{\frac{4}{\pi}}\cdot\hat{v} \tag{4.12}$$

We selected peak 2 for the upcoming calculation for each temperature. Because of the previous chapters 4.1 and 4.3 we know that peak 2 have to be ^{87}Rb and so the mass is $m \approx 1.44322 \cdot 10^{-25}$kg. We have transformed the laser current into frequency as in chapter 4.1 and with the knowledge of σ we get following table:

Temp	ν_0/THz	$y(\nu_0)$/V	σ/MHz	$\hat{v}/\frac{m}{s}$	$\overline{v}/\frac{m}{s}$	T/K	T_{act}/K
24 °C	384.22713	-0.0173	345.26881	269.40	303.98	379.31	297,15
38 °C	384.22737	-0.0313	361.10835	281.75	317.93	414.91	313,15
56.2 °C	384.22724	-0.0482	398.62826	311.03	350.96	505.62	329,35

Table 4.11: fit parameter, velocities and temperature of the gas for each acted temperature

It appears that the calculated temperatures for the gas differs from the acting temperature. But it is worth noticing that the value for σ and so also the doppler width $\Delta\nu_{\mathrm{D}}$ increases with higher temperature. In conclusion to that it gets clear that the scale of the measured values is right and that the transformation from current to frequency once again has cause problems in determine the gas temperature accurately.

Lastly we show in fig. 4.12, 4.13 and 4.14 gaussian fit for each temperature.

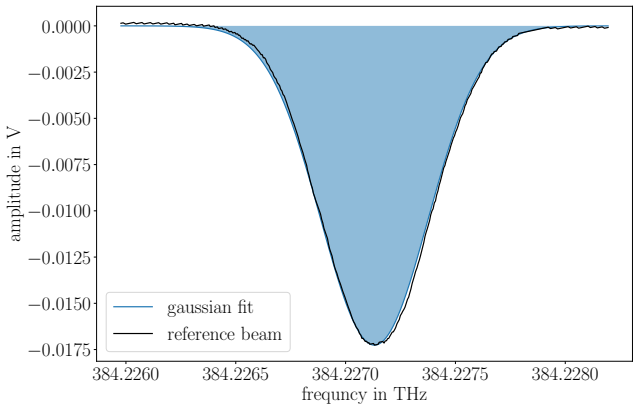

Figure 4.12: gaussian fit for temperature 24 °C

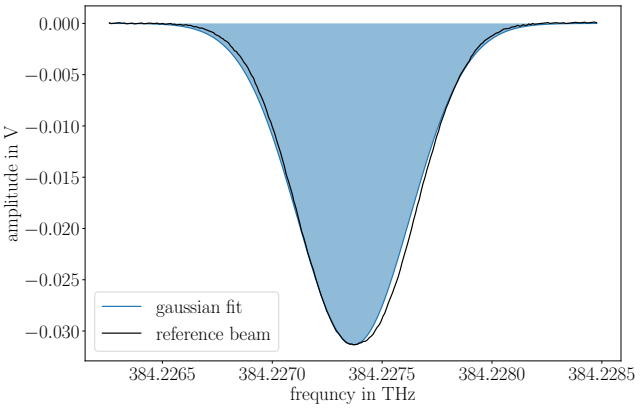

Figure 4.13: gaussian fit for temperature 38 °C

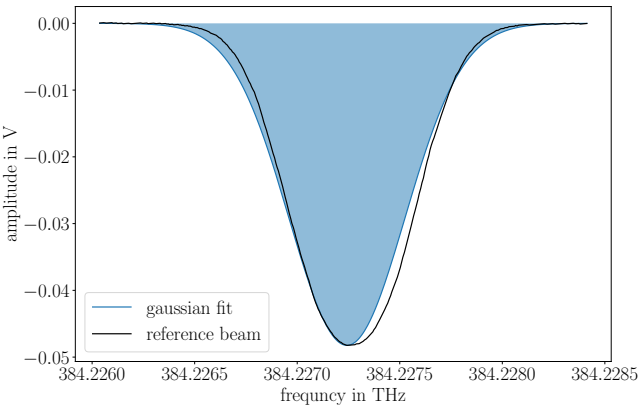

Figure 4.14: gaussian fit for temperature 56.2 °C

5 Closure

In the experiment and the following evaluation of the measured data it becomes clear that the measurement have to be very precisely to detect the small transitions for the hyperfine structure. In the evaluation itself we learned how to fit functions on our measured data, and we get a good overview in the handling of precise measured data.
Overall this experiment gave us a good insight into the topic of saturation spectroscopy and it was a pleasure to see how theory becomes reality.

Bibliography

Bleiner, H. ???? *Versuchsanleitung zum Praktikumsversuch Dopplerfreie Sättigungsspektroskopie von Rubidium*.

Demtröder, W. 2011 *Laserspektroskopie 1*. Springer.

Demtröder, W. 2015 *Experimentalphysik 3*. Springer Spektrum.

Steck, D. 2013 Rubidium 85 d line data.

Steck, D. 2015 Rubidium 87 d line data.